
I Know Kung Fu: Synthetic Dexterous Hand Demonstration Collection via VR Teleoperation

Anonymous Author(s)

Affiliation

Address

email

Abstract

1 **In robotic dexterous manipulation learning, limitations in the acquisition of**
2 **large and scalable amounts of high-quality demonstration data have been a**
3 **critical bottleneck. Although recent works show significant advances in in-**
4 **creasing efficiency through the use of VR technology, human video, or syn-**
5 **thetic demonstration generation techniques, these methods have limitations**
6 **in accuracy and effectiveness. In this project, we propose a data collection**
7 **pipeline that uses a VR-teleoperation system to track human hand motions**
8 **in order to collect dexterous hand demonstrations in simulation. Our method**
9 **utilizes a wrist motion tracker for hand orientation tracking, followed by a**
10 **dexterous retargeting module to sync human movement with robot movement**
11 **in real time. We will also implement demonstration augmentation, ultimately**
12 **yielding multiple distinct, successful trajectories across different scenarios**
13 **from a single human demonstration.**

14 1 Introduction

15 Robotic dexterous manipulation refers to the ability of multi-fingered robotic hands to perform
16 object-centered manipulation tasks. Unlike traditional robot manipulation with claw-like or two-
17 fingered grippers, dexterous manipulation requires precise control of forces and motion similar to
18 human movement.[1].

19 One fundamental problem in robotics is the sim-to-real gap — the misalignment between simulated
20 training and real-world environments due to differences in physics modeling, collision detection,
21 visual rendering, and more. While this gap can be mitigated by enlarging training datasets, dexter-
22 ous manipulation data collection is difficult and expensive. Due to the complexity of multi-jointed
23 dexterous hands that would require extensive training and meticulous reward configuration in RL
24 methods, imitation learning from human demonstrations offers a promising alternative, allowing
25 robots to directly mimic human movement [2, 3]. Previous demonstration collection methods like
26 video extraction prove effective [4, 5, 6] but suffer from poor scalability and significant informa-
27 tion loss during 2D to 3D transformation. Furthermore, many existing data collection pipelines lack
28 cross-embodiment support and only target specific embodiments, which could drastically increase
29 the costs of producing separate, large-scale datasets for different dexterous hand embodiments.

30 To address these issues, we propose a data collection and augmentation pipeline that produces phys-
31 ically plausible, scalable, and generalizable cross-embodiment demonstration data for dexterous
32 manipulation imitation learning. Our pipeline is designed to use VR-teleoperation inspired by
33 OpenVR [7] to collect data in simulation, followed by a data augmentation module inspired by
34 DemoGen [8]. This captures comprehensive physical information while generating tens to hundreds
35 of synthetic demonstrations from a single human example. By varying camera perspective, scene
36 appearance, object models, and robot embodiments, we also effectively increase dataset collection

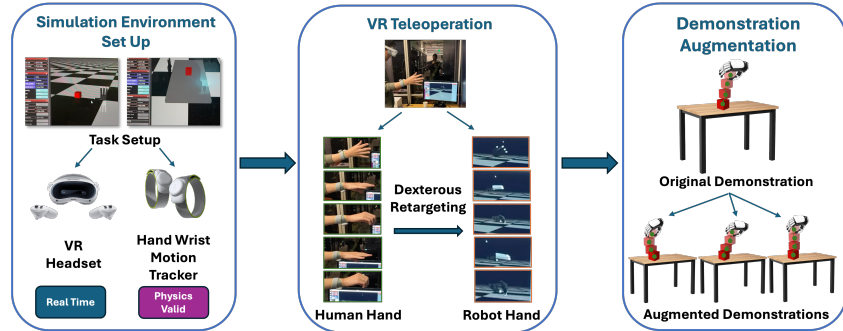


Figure 1: Overview of **I Know Kung Fu** pipeline.

37 scalability. Built on RoboVerse’s [9] unified framework, this system provides cross-simulator and
 38 cross-embodiment support with retargeting capabilities. As a next step, we will fully implement
 39 DemoGen’s demonstration augmentation and P WTF’s [10] filtering modules with VLMs to identify
 40 successful trajectories.

41 **2 Related Work**

42 **2.1 Learning from Human Demonstrations**

43 Imitation learning from human demonstrations effectively trains dexterous hands to complete com-
 44 plex tasks, avoiding complex reward optimization and trial-and-error training in RL techniques.
 45 Traditional imitation learning through video-based demonstration extraction offers high scalability
 46 but loses crucial spatial and physical information during 2D to 3D transformation, producing physi-
 47 cally implausible trajectories. Currently, teleoperation frameworks using gloves, joysticks, or other
 48 controllers, can capture precise trajectories. However, limited by specific teleoperation controllers
 49 and targeted embodiments, they are usually expensive, time-consuming, and hard to scale up.

50 VR-based teleoperation systems advance this by placing operators in simulation environments, cap-
 51 turing universal hand motions that are applicable to various embodiments. This eliminates real robot
 52 setups while ensuring physical plausibility and improving data collection scalability.

53 **2.2 Data Collection via Teleoperation**

54 Teleoperation enables positional data collection through remote robot control, often using equip-
 55 ment like gloves, keyboards, or gamepads. While such teleoperation systems are promising solutions for
 56 bridging sim-to-real gaps and accelerating the training process [2], they become extremely challeng-
 57 ing for multi-fingered dexterous hands due to their complexity.

58 Instead, our work uses a VR teleoperation system inspired by OpenVR [7]. Previous works [11]
 59 have demonstrated VR teleoperation as a promising alternative to conducting imitation learning.
 60 Specifically, this system creates physically plausible training datasets by recording precise action
 61 information and object trajectories. For our pipeline, we leverage dexterous retargeting [12] to
 62 collect dexterous manipulation demonstrations by translating human hand motions to robot motion
 63 in real time through the VR headset.

64 **2.3 Demonstration Augmentation**

65 Demonstration augmentation reduces human effort in training manipulation and visuomotor poli-
 66 cies. One common method of demonstration augmentation includes data generation through the use
 67 of LLMs. LLM-based planning methods can determine optimal trajectories but suffer from hallu-
 68 cinations, action inconsistencies, and a lack of low-level control commands like real physics, joint
 69 angles, and collision detection.

70 MimicGen [13] demonstrates another method by augmenting real, human demonstrations through
 71 spatial transformations, capturing precise human movements to improve learning speed and success

72 rates. Despite these improvements, MimicGen requires expensive on-robot rollouts for visual obser-
 73 vations, limiting scalability. DemoGen [8] advances it by using 3D point clouds and TAMP analysis
 74 instead of visual observation. Thus, its pipeline enables high-speed, cost-effective generation while
 75 decreasing tedious human labor. In our project, we will leverage DemoGen’s advantages as a next
 76 step to augment our collected demonstrations and improve scalability.

77 3 Preliminaries

78 We target a scalable, physics-grounded collection of dexterous-hand demonstrations in simula-
 79 tion with a VR-teleoperation front-end. The system is orchestrated in **RoboVerse** with plug-in-
 80 able physics/rendering back-ends (e.g., IsaacLab/IsaacGym/Genesis/PyBullet/MuJoCo/SAPIEN),
 81 and interfaces to a **Pico 4 Ultra** HMD and an external **motion tracker** through the XR-Robotics
 82 SDK. The operator experiences an egocentric, head-coupled camera in simulation, while the simu-
 83 lator exposes time-synchronized states for the hand root, finger joints, and task objects.

84 **Frames, units, and notation.** We denote by $\mathcal{F}_{\text{pico}}$ the tracking frame (HMD/motion tracker) and
 85 by \mathcal{F}_{sim} the simulator world frame. All linear quantities are in meters, angles in radians, and time in
 86 seconds. The hand root (palm/wrist) pose is $T_{\text{hand}}(t) \in SE(3)$, finger joint vector $q_{\text{finger}}(t) \in R^n$,
 87 and object pose $T_{\text{obj}}(t) \in SE(3)$ at time t . A fixed rigid transform $R_{\text{pico} \rightarrow \text{sim}} \in SO(3)$ maps tracker
 88 coordinates into the simulator world.

89 **Head-coupled camera and logging.** The VR camera extrinsics follow the operator’s head pose to
 90 provide first-person depth and occlusion cues. At each step we log

$$\mathcal{L}(t) = \{T_{\text{hand}}(t), q_{\text{finger}}(t), T_{\text{obj}}(t), \Pi, \Xi(t), \tau(t)\},$$

91 where Π and $\Xi(t)$ are camera intrinsics/extrinsics and $\tau(t)$ is a monotonic timestamp. This schema
 92 enables exact replay and downstream training without additional instrumentation.

93 4 Methods

94 Our method comprises of three modules as shown in the Fig. 1 (i) hand wrist pose tracking in sim-
 95 ulation, (ii) dexterous retargeting via finger motion capture, and (iii) physics-valid demonstration
 96 augmentation. Together they provide real-time VR teleoperation that yields contact-aware trajec-
 97 tories and a data engine for producing large, diverse, and physically plausible demonstrations suitable
 98 for imitation learning.

99 4.1 Hand Wrist Pose Tracking in Simulation

100 The external motion tracker provides a time-stamped 6-DoF signal $(\mathbf{p}_{\text{pico}}(t), \mathbf{q}_{\text{pico}}(t))$ in $\mathcal{F}_{\text{pico}}$. A
 101 fixed rotation $R_{\text{pico} \rightarrow \text{sim}} \in SO(3)$ (estimated once offline during calibration) maps tracker coordi-
 102 nates into the simulator world \mathcal{F}_{sim} . Let \mathbf{q}_R be the unit quaternion associated with $R_{\text{pico} \rightarrow \text{sim}}$ and \otimes
 103 the quaternion product. The hand-root pose applied in simulation is

$$\mathbf{p}_{\text{sim}}(t) = R_{\text{pico} \rightarrow \text{sim}} \mathbf{p}_{\text{pico}}(t), \quad \mathbf{q}_{\text{sim}}(t) = \mathbf{q}_R \otimes \mathbf{q}_{\text{pico}}(t) \otimes \mathbf{q}_R^{-1}, \quad (1)$$

104 and we set $T_{\text{hand}}(t) := (\mathbf{p}_{\text{sim}}(t), \mathbf{q}_{\text{sim}}(t))$ each simulator step. To stabilize closed-loop control, we
 105 constrain the incremental motion by clamping translational and rotational updates to small bounds
 106 (e.g., $\|\Delta \mathbf{p}\| \leq \epsilon_p, \angle(\Delta \mathbf{q}) \leq \epsilon_q$). When tracker frames are dropped or stale, the system skips updates
 107 for that step rather than integrating erroneous samples.

108 Because the VR sensor stream and the simulator may run at different rates, we align them using
 109 nearest-neighbor or linear interpolation in timestamp space. Denoting the simulator step times by
 110 $\{t_k\}$ and the tracker samples by $\{t_i\}$, we compute

$$(\mathbf{p}_{\text{pico}}(t_k), \mathbf{q}_{\text{pico}}(t_k)) \approx \text{Interp}(\{(\mathbf{p}_{\text{pico}}(t_i), \mathbf{q}_{\text{pico}}(t_i))\}_i, t_k),$$

111 followed by (1). A light exponential smoother can be applied on \mathbf{p}_{sim} and \mathbf{q}_{sim} to reduce micro-jitter
 112 while preserving responsiveness. The head pose from the HMD drives an egocentric, head-coupled
 113 camera in the simulator to provide the operator with consistent parallax and occlusion cues. In the
 114 final log $\mathcal{L}(t)$, we store the applied $T_{\text{hand}}(t)$ and the original time-synchronized tracker measurements
 115 for exact replay.

116 4.2 Dexterous Retargeting via Finger Motion Capture

117 Hand landmarks from the XR-Robotics SDK are normalized to a MediaPipe-style skeleton in $\mathcal{F}_{\text{pico}}$
118 and converted at each time step into dexterous joint targets $q_{\text{finger}}(t) \in R^n$ for the simulated hand.
119 The retargeter is configured per embodiment through a specification that lists joint names, ranges,
120 and per-joint scaling factors. In the vector retargeting mode, we first normalize bone lengths and
121 landmark spreads to a canonical scale, then apply a linear mapping with joint-wise clamps:

$$q_{\text{finger}}(t) = \text{Clamp}(W \phi(\text{landmarks}(t)) + b, q_{\text{min}}, q_{\text{max}}),$$

122 where $\phi(\cdot)$ encodes relative landmark directions and apertures, and (W, b) are fitted once from short
123 calibration motions. For digits with coupled kinematics (e.g., distal/proximal phalanges), we enforce
124 simple synergies so that closing motions remain contact-friendly and avoid hyperextension.

125 At each simulator step we send the pair $(T_{\text{hand}}(t), q_{\text{finger}}(t))$ as the position command target. Be-
126 cause contact stabilization in dexterous manipulation is sensitive to small joint oscillations, we op-
127 tionally add a first-order low-pass filter on $q_{\text{finger}}(t)$ and saturate velocity/acceleration changes to
128 remain within the physical capabilities of the simulated hand. The operator receives immediate
129 visual feedback through the head-coupled view, which empirically reduces overshoot near contact
130 initiation. The log $\mathcal{L}(t)$ records $T_{\text{hand}}(t)$, $q_{\text{finger}}(t)$, the object pose $T_{\text{obj}}(t) \in SE(3)$, and camera
131 parameters, all time-stamped for downstream learning and analysis.

132 5 Discussion and Future Work

133 **Motivation and design rationale.** We aim for a *scalable, generalizable* pathway to dexterous ma-
134 nipulation data. VR teleoperation captures human hand motion at fine spatiotemporal resolution and
135 maps it, in real time, to simulator-native trajectories $\{T_{\text{hand}}(t), q_{\text{finger}}(t)\}$. To make seeds portable
136 across embodiments, we also maintain a canonical human-hand parameterization and learn a retar-
137 geter per robot hand. Using **RoboVerse** separates task orchestration from physics/rendering and
138 headset I/O, positioning the pipeline for *cross-VR* (different HMDs/trackers) and *cross-simulator*
139 (MuJoCo/Isaac/SAPIEN) reuse without changing the logging schema. The resulting seeds are
140 contact-rich, physics-valid, and ready for augmentation and policy learning.

141 **Toward scalable augmentation.** We will integrate a DemoGen-style inference module to expand
142 seeds without extra teleoperation. A source trajectory is decomposed into *on-object skill* (contact)
143 and *free-space* segments; the former are transformed coherently to preserve contact frames, while the
144 latter are re-planned under new scene configurations so kinematics and collisions remain feasible.
145 Visual observations are synthesized in a point-cloud modality by rearranging subjects via 3D editing,
146 keeping action intent aligned to novel object configurations. We will sample *multiple* variants along
147 object-pose resets, object instances, viewpoints, and small timing/pose disturbances, accepting only
148 those that satisfy the seed’s task predicates. The augmented set uses the same units and notation as
149 $\{T_{\text{hand}}(t), q_{\text{finger}}(t), T_{\text{obj}}(t)\}$.

150 **Experimental plan.** (i) *Cross-VR reproducibility*: collect with different headsets/trackers; re-
151 port fingertip error and DTW of contact sequences, plus user-time \rightarrow usable-demo throughput.
152 (ii) *Cross-simulator portability*: replay identical seeds across engines; report terminal object er-
153 ror $\|T_{\text{obj}}^{\text{final}} - T_{\text{obj}}^{\text{goal}}\|$, contact-event alignment, and success gaps. (iii) *Augmentation scaling*: with the
154 Demonstration Augmentation module enabled, plot success versus reset coverage and dataset size;
155 ablate pose/instance/viewpoint/disturbance sampling; compare BC/Diffusion policies trained on one
156 seed vs. seeds+augmented.

157 **Limitations and open problems.** VR introduces noise, latency, and frame drops that can cause
158 micro-oscillations in $q_{\text{finger}}(t)$; smoothing and rate limits help but may not eliminate artifacts.
159 MANO-to-robot retargeting can distort contact geometry for disparate kinematics; per-embodiment
160 calibration and contact-aware synergies are needed. Cross-simulator replay may shift contact tim-
161 ing; we will quantify and, if necessary, constrain tasks to regimes where engines agree. Augmen-
162 tation can bias resets toward easy regions if acceptance is too strict; coverage heatmaps and tuned
163 sampling/validation will counteract mode collapse. Despite these caveats, VR-in-sim seeds plus
164 DemoGen-style expansion offer a principled route to scalable, generalizable dexterous datasets.

References

- 165
166 [1] A.M. Okamura, N. Smaby, and M.R. Cutkosky. An overview of dexterous manipulation. In
167 *Proceedings 2000 ICRA. Millennium Conference. IEEE International Conference on Robotics*
168 *and Automation. Symposia Proceedings (Cat. No.00CH37065)*, volume 1, pages 255–262
169 vol.1, 2000.
- 170 [2] Gaofeng Li, Ruize Wang, Peisen Xu, Qi Ye, and Jiming Chen. The developments and chal-
171 lenges towards dexterous and embodied robotic manipulation: A survey, 2025.
- 172 [3] Shan An, Ziyu Meng, Chao Tang, Yuning Zhou, Tengyu Liu, Fangqiang Ding, Shufang Zhang,
173 Yao Mu, Ran Song, Wei Zhang, Zeng-Guang Hou, and Hong Zhang. Dexterous manipulation
174 through imitation learning: A survey, 2025.
- 175 [4] Georgios Pavlakos, Dandan Shan, Ilija Radosavovic, Angjoo Kanazawa, David Fouhey, and
176 Jitendra Malik. Reconstructing hands in 3d with transformers, 2023.
- 177 [5] Han Zhang, Songbo Hu, Zhecheng Yuan, and Huazhe Xu. Doglove: Dexterous manipulation
178 with a low-cost open-source haptic force feedback glove. *arXiv preprint arXiv:2502.07730*,
179 2025.
- 180 [6] Philipp Wu, Yide Shentu, Zhongke Yi, Xingyu Lin, and Pieter Abbeel. Gello: A general,
181 low-cost, and intuitive teleoperation framework for robot manipulators, 2023.
- 182 [7] Abraham George, Alison Bartsch, and Amir Barati Farimani. Openvr: Teleoperation for ma-
183 nipulation, 2023.
- 184 [8] Zhengrong Xue, Shuying Deng, Zhenyang Chen, Yixuan Wang, Zhecheng Yuan, and Huazhe
185 Xu. Demogen: Synthetic demonstration generation for data-efficient visuomotor policy learn-
186 ing. *arXiv preprint arXiv:2502.16932*, 2025.
- 187 [9] Haoran Geng, Feishi Wang, Songlin Wei, Yuyang Li, Bangjun Wang, Boshi An, Char-
188 lie Tianyue Cheng, Haozhe Lou, Peihao Li, Yen-Jen Wang, Yutong Liang, Dylan Goetting,
189 Chaoyi Xu, Haozhe Chen, Yuxi Qian, Yiran Geng, Jiageng Mao, Weikang Wan, Mingtong
190 Zhang, Jiangran Lyu, Siheng Zhao, Jiazhao Zhang, Jialiang Zhang, Chengyang Zhao, Hao-
191 ran Lu, Yufei Ding, Ran Gong, Yuran Wang, Yuxuan Kuang, Ruihai Wu, Baoxiong Jia, Carlo
192 Sferazza, Hao Dong, Siyuan Huang, Yue Wang, Jitendra Malik, and Pieter Abbeel. Robo-
193 verse: Towards a unified platform, dataset and benchmark for scalable and generalizable robot
194 learning, 2025.
- 195 [10] Chuanruo Ning, Kuan Fang, and Wei-Chiu Ma. Prompting with the future: Open-world model
196 predictive control with interactive digital twins, 2025.
- 197 [11] Tianhao Zhang, Zoe McCarthy, Owen Jow, Dennis Lee, Xi Chen, Ken Goldberg, and Pieter
198 Abbeel. Deep imitation learning for complex manipulation tasks from virtual reality teleoper-
199 ation, 2018.
- 200 [12] Yuzhe Qin, Wei Yang, Binghao Huang, Karl Van Wyk, Hao Su, Xiaolong Wang, Yu-Wei Chao,
201 and Dieter Fox. Anyteleop: A general vision-based dexterous robot arm-hand teleoperation
202 system. In *Robotics: Science and Systems*, 2023.
- 203 [13] Ajay Mandlekar, Soroush Nasiriany, Bowen Wen, Iretiayo Akinola, Yashraj Narang, Linxi Fan,
204 Yuke Zhu, and Dieter Fox. Mimicgen: A data generation system for scalable robot learning
205 using human demonstrations. In *7th Annual Conference on Robot Learning*, 2023.